Importance Sampling and Feature Fusion Paradigm-Boosted Multi-Modal Convolutional Neural Networks

Deployment in Composite Curing Process Monitored by Electro-Mechanical Impedance

Gao, Zeyuan; Zhao, Xin; Li, Meng; Han, Zhibin; Zhu, Jianjian

DOI
10.1109/ACCESS.2025.3551508

Publication date
2025

Document Version
Final published version

Published in
IEEE Access

IEEE Access
Multidisciplinary : Rapid Review : Open Access Journal

Received 3 January 2025, accepted 16 February 2025, date of publication 17 March 2025, date of current version 26 March 2025.

Digital Object Identifier 10.1109/ACCESS.2025.3551508

RESEARCH ARTICLE

Importance Sampling and Feature Fusion Paradigm-Boosted Multi-Modal Convolutional Neural Networks: Deployment in Composite Curing Process Monitored by Electro-Mechanical Impedance

XIN ZHAO[1], ZEYUAN GAO[1], MENG LI[1], ZHIBIN HAN[2], AND JIANJIAN ZHU[1]

[1]College of Aviation Engineering, Civil Aviation Flight University of China, Guanghan 618307, China
[2]Faculty of Aerospace Engineering, Delft University of Technology, 2629 HS Delft, The Netherlands

Corresponding author: Jianjian Zhu (zhujj.work@cafuc.edu.cn)

This work was supported in part by the Young Scientist Fund of the National Natural Science Foundation of China under Grant 52205171, and in part by the Targeted Support from Civil Aviation Flight University of China for the Introduction of High-Level Talents under Grant CZKY2024209.

ABSTRACT The increasing application of composite materials in various industrial sectors is driven by their lightweight nature, high strength-to-stiffness ratio, and corrosion resistance. Effective monitoring of the curing process is crucial for ensuring quality and performance. Electro-Mechanical Impedance (EMI) offers promising, non-destructive, real-time monitoring, but the complexity of EMI signals poses challenges. Convolutional Neural Networks (CNNs) have the potential to enhance EMI-based monitoring accuracy. However, training CNNs on multi-modal EMI signals requires addressing data heterogeneity, class imbalance, and computational complexity at present. This study develops the Importance Sampling Algorithm-optimized Multi-Modal CNNs (ISA-MM-CNNs) paradigm for EMI-based evaluation of composite curing processes. By prioritizing informative samples and capturing complementary information from diverse EMI signal modalities, we aim to improve the robustness and efficiency of CNNs in evaluating curing degrees. This study outlines EMI monitoring challenges, details the ISA-MM-CNNs paradigm, and discusses data preprocessing, network architecture, and training optimization. Experimental results demonstrate the superiority of the developed ISA-MM-CNNs and suggest further studies for the curing monitoring of composites.

INDEX TERMS Composite curing, convolutional neural networks, electro-mechanical impedance, importance sampling algorithm, multi-modal learning.

I. INTRODUCTION

The employment of composite materials in various industrial sectors has garnered increasing attention due to their lightweight, high strength-to-stiffness ratio, and corrosion-resistant properties [1], [2]. Evaluating the curing process of composite structures is essential to ensure their quality and service performance. Electro-Mechanical Impedance (EMI) has emerged as a promising approach for evaluating the curing process [3], offering advantages such as non-destructive evaluation and sensitivity to changes in material properties [4]. However, the complex and multi-modal attribute of EMI signals poses a significant challenge to accurate and efficient monitoring.

Recent advancements in the integration of EMI, convolutional neural networks (CNNs), and composite structures have significantly facilitated the development of the structural health monitoring (SHM) community [5], [6]. The EMI

The associate editor coordinating the review of this manuscript and approving it for publication was Ghufran Ahmed.

method, utilizing piezoelectric sensors, is effective for early damage detection by measuring electrical impedance changes in structures [5]. This technique has been enhanced by incorporating deep learning models, such as the CNNs mentioned above, to analyze data collected from sensors and predict structural signatures [7], [8], [9], [10]. For instance, EMI data processed with deep learning models are capable of assessing structural strength and detecting pitting corrosion damage [11], [12], [13]. CNNs are particularly valuable in SHM due to their ability to extract and classify features from raw sensor data automatically. They have been used to convert ultrasonic signals from impact events on composite structures into 2D images, achieving high accuracy in detecting and localizing impacts [14], [15], [16], [17]. Additionally, composite materials, like fiber-reinforced polymers (FRPs), benefit from SHM systems that use embedded sensors and advanced data analysis techniques to detect barely visible impact damage (BVID) [18], [19], [20], [21], [22]. A notable development is the convolutional neural networks Long Short-Term Memory (CNN-LSTM) hybrid model, which combines the spatial feature extraction of CNNs with the temporal sequence learning of LSTMs to predict EMI signals and monitor bond strength in composite structures [23], [24], [25], [26], [27]. This integration of EMI with CNNs offers enhanced capabilities for damage detection, localization, and characterization, ensuring the reliability and safety of composite structures in various engineering applications.

To address the above-mentioned challenges and further promote the development of the field based on the existing academic efforts, this study proposes an ensemble approach, which is the Importance Sampling Algorithm (ISA)-optimized Multi-Modal Convolutional Neural Networks (ISA-MM-CNNs) paradigm for EMI-based curing process monitoring of composite structures. The proposed paradigm integrates the advantages of importance sampling algorithms, which focus training efforts on informative samples [28], [29], [30], with multi-modal learning methods to capture complementary information from different EMI signal modalities effectively. By exploiting the inherent structure of EMI signals and optimizing the training process driven by the importance sampling algorithm, the proposed paradigm aims to improve the robustness and efficiency of CNNs for the application of curing degree evaluation.

In this study, an overview of EMI-based deep learning and the challenges associated with multi-modal signal analysis is provided and employed in the field of composite structures. The proposed ISA-MM-CNNs paradigm is then introduced, and its key components, including data preprocessing, network architecture design, and training optimization strategies, are discussed. Furthermore, results demonstrating the effectiveness and superiority of the proposed paradigm compared to existing approaches are presented. Finally, this paper discusses further studies in the field of composite structures monitoring by integrating ISA-MM-CNNs with the EMI method.

II. METHODOLOGY OF ISA–OPTIMIZED MM-CNNs

A. FUNDAMENTAL OF IMPORTANCE SAMPLING ALGORITHM

Importance sampling is a statistical method employed to estimate properties of a target probability distribution by leveraging samples generated from a distinct, more tractable distribution, often referred to as the proposal distribution. This technique proves particularly useful in situations where direct sampling from the target distribution is either computationally burdensome or impractical. The underlying principle of importance sampling involves reweighting the samples drawn from the proposal distribution to approximate expectations with respect to the target distribution [31], [32].

Given a target probability density function $p(x)$ and a proposal probability density function $q(x)$, the goal of importance sampling is to estimate the expected value of a function $f(x)$ with respect to $p(x)$, as given by *(1)*:

$$E_P[f(x)] = \int f(x)p(x)dx \tag{1}$$

Since directly sampling from $p(x)$ may be difficult, we instead draw samples $x_1, x_2, \ldots, x_n$ from the proposal distribution $q(x)$. To account for the fact that these samples are not drawn from $p(x)$, the importance weights $w(x)$ is employed, defined as *(2)*:

$$w(x) = \frac{p(x)}{q(x)} \tag{2}$$

The samples from $q(x)$ can be reweighted to approximate the expectation under $p(x)$ by applying the *(3)*:

$$\begin{aligned} E_p\left[f\left(x\right)\right] &= \int f\left(x\right)p\left(x\right)dx \\ &= \int f\left(x\right)\frac{p\left(x\right)}{q\left(x\right)}q\left(x\right)dx \\ &= \int f\left(x\right)w\left(x\right)q\left(x\right)dx \end{aligned} \tag{3}$$

The steps involved in importance sampling are straightforward. First of all, select a proposal distribution $q(x)$ from which it is easy to draw samples. This distribution should have support that covers the support of the target distribution $p(x)$. Secondly, generate a set of samples $x_1, x_2, \ldots, x_n$ from the proposal distribution $q(x)$. Then, the importance weights $w\left(x_i\right) = p\left(x_i\right)/q\left(x_i\right)$ for each sample are to be calculated. Lastly, employing the weighted average of the function $f(x)$ over the samples can estimate the expectation with respect to $p(x)$, as described by *(4)*:

$$E_p\left[f\left(x\right)\right] \approx \frac{1}{n}\sum\nolimits_{i=1}^{n} f\left(x\right)w\left(x_i\right) \tag{4}$$

Importance sampling has several benefits and challenges. It can be more efficient than direct sampling from the target distribution, especially in the case of a complex target distribution. Additionally, the method is flexible and can be applied to various types of integrals and distributions. However, it is crucial to select an appropriate proposal distribution. A poor choice can lead to high variance in the importance weights, making the estimator unreliable. To eliminate this problem, it is helpful to normalize the weights to prevent numerical instability, as shown in (5):

$$\hat{w}\left(x_i\right) = \frac{w\left(x_i\right)}{\sum_{j=1}^{n} w\left(x_j\right)} \tag{5}$$

By employing normalized weights, the expectation estimate is yielded as (6):

$$E_p\left[f\left(x\right)\right] \approx \sum\nolimits_{i=1}^{n} \hat{w}\left(x_i\right) f\left(x_i\right) \tag{6}$$

To sum up, importance sampling is a powerful statistical technique used in various fields to approximate difficult integrals and estimate posterior distributions. It is essential in Monte Carlo integration, Bayesian inference, and simulations of complex systems in physics and engineering [31]. By sampling from an easier distribution and reweighting those samples to reflect the target distribution, importance sampling effectively approximates expectations and integrals. The broad application of the importance sampling method depends on carefully choosing the proposal distribution and managing the variance of the importance weights, making it a robust method across diverse applications [33]. The flowchart of the importance sampling algorithm is depicted in

B. FUNDAMENTALS OF MULTI-MODAL CONVOLUTIONAL NEURAL NETWORK

Multi-Modal Convolutional Neural Networks (MM-CNNs) are specialized neural network architectures designed to integrate and process multiple image datasets that share a similar nature or domain, such as different kinds of data from various sources [34], [35]. However, in this study, a homogeneous multi-modal learning framework is designed, which employs image datasets from different scenarios. The approach developed in this study aims to leverage the complementary information inherent in these similar but distinct datasets to improve the overall performance of image recognition, classification, or other image-processing tasks [20].

Specifically, the classification of images is the objective task mentioned in this study. The core components of MM-CNNs include feature extraction pipelines for each image dataset, feature fusion mechanisms to combine the extracted features, and attention mechanisms to dynamically weigh the importance of features from different datasets. Feature extraction typically involves convolutional layers tailored to the characteristics of each dataset. For each image dataset $X(i)$, the convolutional layers extract feature maps $F(i)$ via (7):

$$F_{i,j,k}^{(i)} = \sigma\left(\sum\nolimits_{m=0}^{M-1} \sum\nolimits_{n=0}^{N-1} \sum\nolimits_{c=0}^{C-1} W_{m,n,c,k}^{(i)} \cdot X_{i+m,j+n,c}^{(i)} + b_k^{(i)}\right) \tag{7}$$

where $F$is the output feature map for the i-th dataset, σ is the activation function, $W(i)$ and $b(i)$ are the convolutional filters and biases for the i-th dataset, and $X(i)$ is the input image from the i-th dataset.

The mathematical formulation of MM-CNNs designed in this study involves several key steps. For each image dataset, convolutional layers extract feature maps, which can then be fused using techniques such as concatenation, addition, or more complex operations. In this study, the fusion occurs at the late stage in terms of the design of the network. The combined feature maps can be represented as (8):

$$F_{\text{fused}} = \text{Fusion}(F^{(1)}, F^{(2)}, \ldots, F^{(N)}) \tag{8}$$

where N is the number of image datasets. Private layers can be used to capture dataset-specific features, as expressed in (9):

$$F_{\text{private}}^{(i)} = \sigma\left(W_{\text{private}}^{(i)} \cdot F^{(i)} + b_{\text{private}}^{(i)}\right) \tag{9}$$

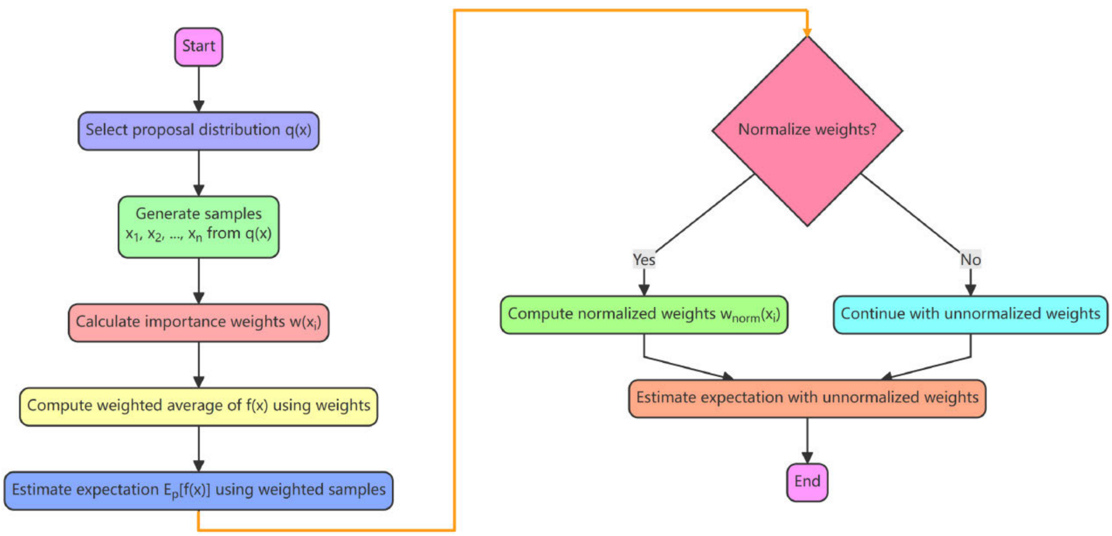

FIGURE 1. Flowchart of the importance sampling algorithm.

while shared layers promote common feature learning across datasets, as presented in (10):

$$F_{\text{shared}} = \sigma\left(W_{\text{shared}} \cdot F_{\text{fused}} + b_{\text{shared}}\right) \tag{10}$$

An attention mechanism can be applied to dynamically weigh the importance of features from each dataset, enhancing the fusion process. This attention mechanism calculates weights for the features of each dataset based on their relevance, as given by (11):

$$\alpha^{(i)} = \frac{e^{score\left(F^{(i)}\right)}}{\sum_{j=1}^{N} e^{score\left(F^{(j)}\right)}} \tag{11}$$

The fused features $F_{\text{fused\_att}}$ with attention can be given by (12):

$$F_{fused\_att} = \sum_{i=1}^{N} \alpha^{(i)} F^{(i)} \tag{12}$$

The result is a set of fused features that integrate information from all datasets, leveraging their complementary strengths to improve the model performance. MM-CNNs have significant applications and benefits across various fields. By effectively extracting and fusing features from multiple image datasets, MM-CNNs achieve superior performance in diverse image processing tasks, demonstrating the importance of proper feature extraction pipelines, fusion mechanisms, and attention mechanisms.

C. FRAMEWORK OF MULTI-MODAL CONVOLUTIONAL NEURAL NETWORKS

From the perspective of building the MM-CNNs model, the framework of the proposed model includes the convolutional layers, pooling layers, flattened layers, concatenation layers, attention layers, dropout layers, and fully connected layers. Specifically, the framework of the MM-CNNs is designed to effectively integrate multi-modal data, allowing the model to capture and leverage the unique features from different data sources. The framework of the proposed MM-CNNs model is depicted in. The convolutional layers are employed to extract spatial hierarchies of features from the input data automatically. Pooling layers are incorporated to reduce the dimensionality of feature maps, thereby controlling overfitting and enhancing computational efficiency. After the above operations, the data is passed through flattened layers to transform the pooled feature maps into a vector form that is suitable for further processing. Concatenation layers play a critical role in the MM-CNNs framework, enabling the integration of features extracted from multiple modalities. This integration facilitates a comprehensive understanding of the data by combining complementary information from different sources.

Following concatenation, the data is processed through fully connected layers accompanied by the inserted dropout layers, which perform high-level reasoning and ultimately produce the output of the model. These layers are essential for learning complex patterns and relationships within the data. Additionally, regularization techniques such as dropout can be applied in these layers to prevent overfitting. Overall, the MM-CNNs framework is meticulously designed to harness the power of convolutional neural networks for multi-modal data, ensuring robust feature extraction, integration, and interpretation, which leads to the promoted performance on tasks requiring the fusion of diverse data types.

D. DEPLOYING ISA TO OPTIMIZE THE HYPERPARAMETERS OF MM-CNNs

As aforementioned, importance sampling is a technique used to optimize the hyperparameters of MM-CNNs by improving the efficiency of the training process. The core idea is to sample hyperparameter values from a distribution that emphasizes more promising regions of the hyperparameter space rather than sampling uniformly. This helps in focusing

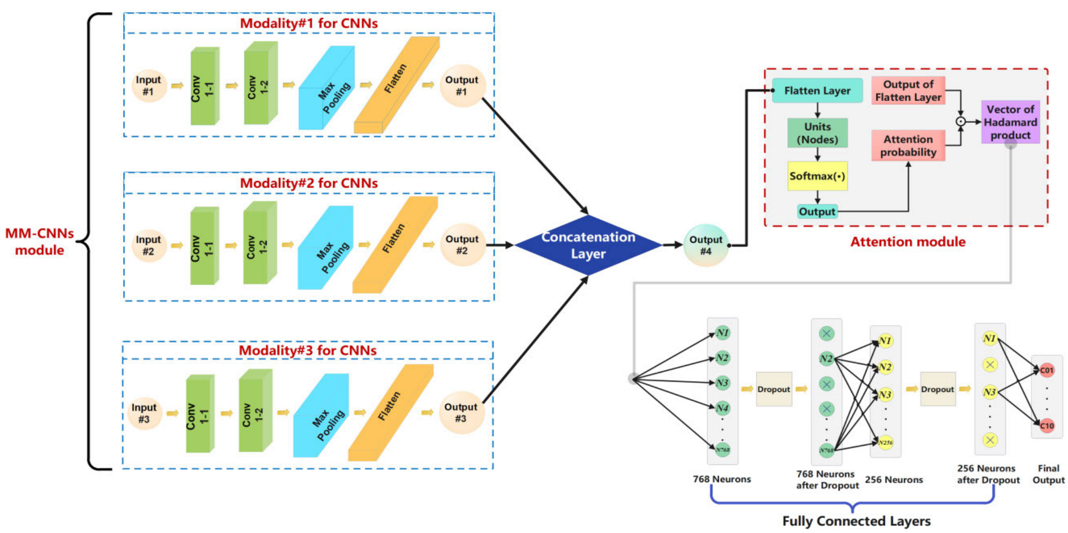

FIGURE 2. Schematic of the proposed MM-CNNs framework.

computational resources on hyperparameters that are more likely to yield better performance. The probability density function (PDF) used for sampling is adjusted iteratively based on the performance of previously sampled hyperparameters.

Optimizing MM-CNNs using the importance sampling algorithm involves several critical steps aimed at enhancing the efficiency and effectiveness of the training process. Initially, the weights of the model and hyperparameters are set, and the multi-modal data is preprocessed to ensure compatibility with the network. This data is then split into training and testing sets, with the training set employed to teach the model and the testing set reserved for performance evaluation. The key to this approach is computing importance sampling weights based on the losses from previous epochs, assigning higher weights to more informative samples. Formally, the importance sampling weight w_i for a sample i is computed by *(13)*:

$$w_i = \frac{L_i^{\alpha}}{\sum_j L_j^{\alpha}} \tag{13}$$

where L_i represents the loss for sample i from a previous epoch, and α is a hyperparameter that controls the degree of prioritization. By focusing on samples with higher weights, the model can learn more effectively from data that has a greater impact on reducing overall error, thereby optimizing the learning process.

During the training process, the model undergoes iterative forward and backward passes. In the forward pass, predictions $\hat{y}$ are made, and the loss $L$for each sample is calculated using a suitable loss function, such as cross-entropy loss for classification tasks, as shown in *(14)(14)(14)*:

$$L = -\sum_{c} y_c \log\left(\hat{y}_c\right) \tag{14}$$

where y_c is the true label and $\hat{y}_c$ is the predicted probability for class c. In the backward pass, gradients of the loss with respect to the model parameters θ are computed, and the parameters are updated using the weighted losses, as given by *(15)*:

$$\theta_{t+1} = \theta_t - \eta \sum_{i}^{w_i \nabla\theta L_i} \tag{15}$$

where η is the learning rate, and $\nabla\theta L_i$ is the gradient of the loss for sample I with respect to the parameters. The importance sampling weights w_i ensure that the updates are more influenced by the samples that have the most significant losses, thus directing the model learning focus towards the most critical data points.

Regular evaluation of the testing set helps monitor the model performance and detect overfitting. If the model has not yet converged, the importance sampling weights are recalculated, and training continues. Importance sampling method significantly accelerates convergence by focusing the learning process on the most impactful samples, thereby improving the overall effectiveness and efficiency of the MM-CNNs model. This approach leverages the principle that not all samples contribute equally to the learning process, allowing the model to allocate its learning resources more judiciously.

III. EXPERIMENTAL SETUP AND DATASET DESCRIPTION

A. EXPERIMENTAL SETUP AND ORIGINAL DATA ACQUISITION

Experiments are devised and executed to authenticate the proposed methodology outlined in this study. The specimens comprise ten plies with the stacking sequence $[(0,90)]_{10}$. The composite patch dimensions are 100 mm×100 mm×2 mm, alongside a 300 mm×300 mm×3 mm aluminum plate utilized in both setups. Sensor-wise, the specimens integrated a piezoelectric wafer with 6 mm in diameter and 0.5 mm in thickness. Table 1 outlines the specifications for an experimental configuration involving composite materials and sensor instrumentation.

TABLE 1. Specification of samples used in experiments.

ITEMS	SPECIMENS USED IN EXPERIMENTS
PLY NUMBER	10
PLY SEQUENCE	[(0,90)]10
OVERALL SIZE (L×W×T)	PATCH SIZE: 100 MM×100 MM×2 MM PLATE SIZE: 300 MM×300 MM×3 MM
PIEZOELECTRIC WAFER	DIAMETER: 6 MM THICKNESS: 0.5 MM

Experiments carried out in the laboratory are aimed at assessing the curing process of composite structures utilizing EMI. This specimen represents a co-cured structure, combining both composite and metallic components. For clarity, the setup for EMI measurement and the fabricated samples are depicted in Fig. 4. Fig.4 (a) depicts a testing platform, which is composed of a WK6500B impedance analyzer made by Wayne Kerr Electronics Ltd, London, a PC controller, and a heating device. The impedance analyzer is connected to the piezoelectric wafer via heat-resistant wires, which facilitates data acquisition throughout the entire curing process. The PC controller is employed to modulate the frequency scope with a step of 1 kHz. Fig.4 (b) shows the overall size of the specimen used in the experiment, which is integrated with a piezoelectric wafer. The curing process duration spans approximately 240 minutes, with data sampling conducted at intervals of 2 minutes, resulting in the acquisition of 121 groups of raw data.

In the end, the dataset is constructed in our laboratory, which is composed of original data measured by the EMI method in the curing process of the co-cured structure. Specifically, the authors named this dataset "CS_CURE_EMI700", which means the upper and the lower frequencies ranging from 100 to 700 kHz in the process of composite fabrication. The curve plots using the "CS_CURE_EMI700" are shown in Fig.5. For the purpose of the intelligent model application, the "CS_CURE_EMI700" is divided into ten classes, ranging from C01 to C10 in terms of the curing degree indicator, which is the Root Mean Square Deviation (RMSD).

B. IMAGES CONVERTED FROM ORIGINAL DATA

Considering the proposed ISA-MM-CNNs approach deployed in this study is based on the two-dimensional CNNs, thus the input shape of the proposed approach requires the image format. In this section, the numeric data in the "CS_CURE_EMI700" dataset is converted to images with the methods of Recurrence Plots (RP), Markov Transition Field (MTF), and Gramian Angular Field (GAF). Transforming numeric data into image representations using the above three methods can bring the advantages of capturing nonlinear features, state transitions, and global information for intuitive pattern recognition and analysis.

Owing to the difficulty of showing all the transformed GAF images in one paper at the same time, only the GAF, RP, and MTF images using the dataset of "CS_CURE_EMI700" at the initial and final stages during the curing process are represented in Fig. 6. Comparatively, the subgraphs of Fig. 6 illustrate that the transformed images exhibit distinct features. The constructed "CS_CURE_EMI700" dataset, comprising data with a dimensionality of 700, yields a visual representation with 700 pixels in both horizontal and vertical directions in GAF images. Notably, an inspection of the GAF images discloses a distinct cruciform pattern, which correlates with the peak frequency observed in Fig. 5, suggesting the association between these two phenomena.

Similarly, RP images are a visualization method used to analyze the behavior of one system over time, while MTF images visualize the dynamics of one system with discrete states by showing how likely it is for the system to transition from one state to another. Therefore, both methods can help identify patterns and attractors in the curing process of composite structures, providing valuable insights into the behavior of the curing process. The RP and MTF images are presented in Fig. 6 with distinct features at the initial and final states of the curing process. According to these RP and MTF images shown in Fig. 6 (a) and (b), it can be inferred that the curing process induces notable transformations in the material composition and arrangement from these images, influencing its mechanical properties and performance characteristics.

C. DATASET CONSTRUCTION AND SPLITTING

Although substantial effort has been made in CNNs-related studies for composites in previous studies, the scarcity of high-quality data remains a significant impediment to the development of sophisticated models capable of achieving accurate predictions. To address this limitation, the Synthetic Minority Over-sampling Technique (SMOTE) is employed in this study. This theoretically grounded and empirically validated methodology utilizes the originally obtained EMI data to synthetically generate additional samples, augmenting the size of the training dataset. This study ultimately enables the development of more robust and reliable ISA-MM-CNNs by enhancing the quality and quantity of available training data.

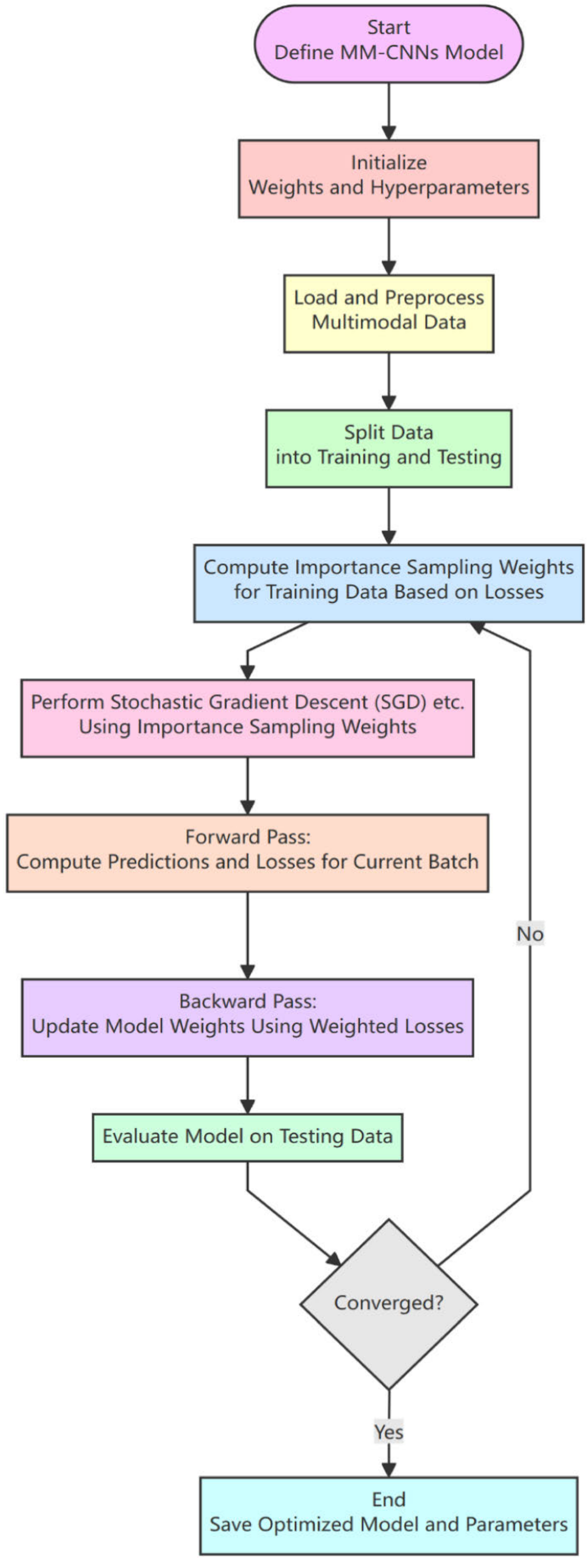

FIGURE 3. Flowchart of optimizing MM-CNNs hyperparameters using importance sampling algorithm.

As previously noted, the initially acquired resistance data are subject to an initial expansion phase, followed by a

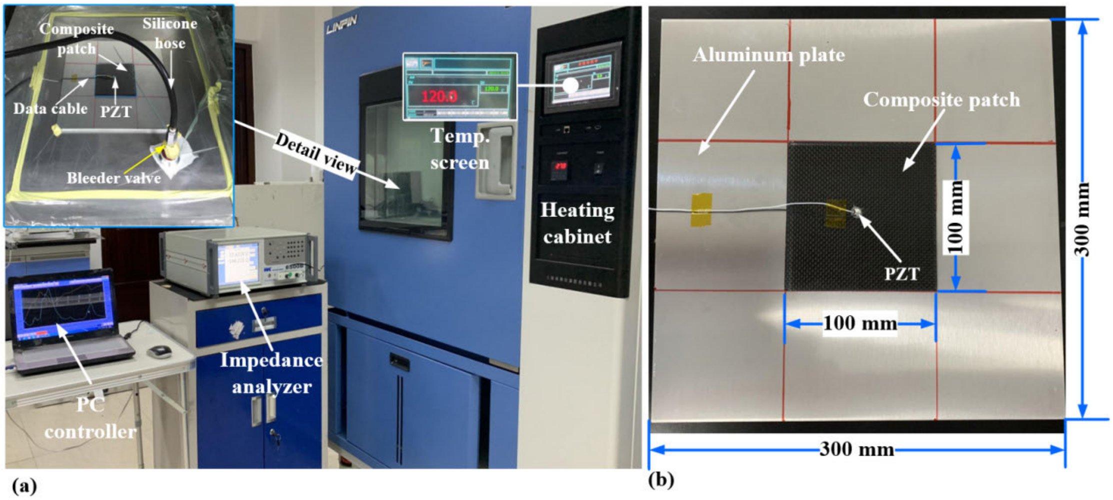

FIGURE 4. Platform for EMI testing in curing monitoring: (a) overall view, (b) co-cured specimen.

TABLE 2. Hyperparameters to evaluate the influence on ISA-MM-CNNs performance.

Items	Space	HC1	HC2	HC3	HC4	HC5	HC6	HC7	OHP
DR	[0.21, 0.39]	0.23	0.33	0.31	0.37	0.29	0.37	0.21	0.21
LR	[10^{-4}, 10^{-3}]	1×10^{-4}	2×10^{-4}	9×10^{-4}	6×10^{-4}	9×10^{-4}	1×10^{-3}	1×10^{-4}	7×10^{-4}
Batch	[8, 16, 32, 64]	8	8	16	16	32	32	64	64

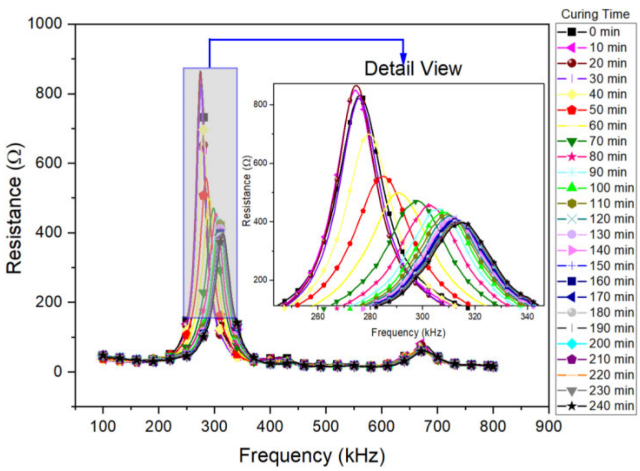

FIGURE 5. Curve plots using the original data in the "CS_CURE_EMI700" dataset.

transformation process yielding a comprehensive dataset with multi-modal features, including GAFs, RP, and MTF images. The resultant image dataset comprised a total of 681 samples, enriching the data and facilitating subsequent analysis. Notably, the transformed image dataset is subsequently categorized into 10 distinct classes, each corresponding to a specific impact energy level.

Within the image dataset converted from the "CS_CURE_EMI700" dataset, a stratified sampling strategy is employed, wherein 80% of the total samples are designated for model training and 10% for model validation, while the remaining 10% are reserved for testing purposes, as depicted in Fig. 7. Furthermore, to ensure optimal model performance and alleviate potential biases in the training process, all samples, utilized for both ISA-MM-CNNs fitting, are randomly shuffled and re-ordered to enhance trainability, foster convergence, and ultimately optimize the fitting of the customized ISA-MM-CNNs model to the underlying data distribution.

IV. RESULTS AND DISCUSSION

A. IMPACT OF HYPERPARAMETERS ON ISA-MM-CNNs PERFORMANCE

The performance of ISA-MM-CNNs with optimal architecture is heavily influenced by the choice of hyperparameters, such as the number of modalities used, the size and number

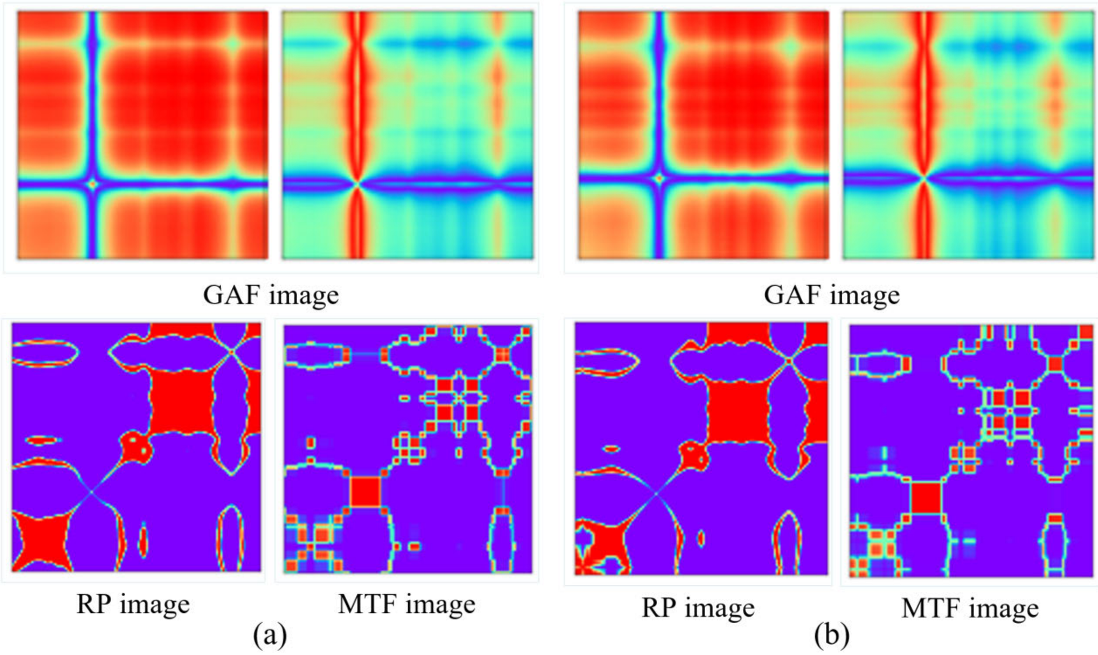

FIGURE 6. Converted images using the "CS_CURE_EMI700" dataset: (a) initial state, (b) final state.

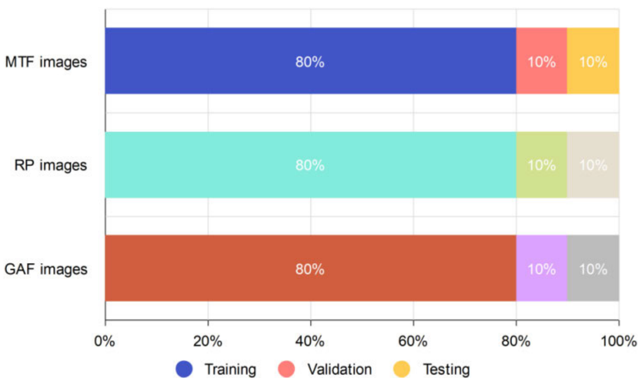

FIGURE 7. Splitting of the converted image dataset for ISA-MM-CNNs fitting.

of filters in convolutional layers, the number of fully connected layers, and the learning rate. These hyperparameters can significantly impact the ability of the model to classify images from multiple modalities accurately. In addition to these individual hyperparameters, the interplay between them can have a compounding effect on the overall performance of the ISA-MM-CNNs.

Considering that optimizing the massive hyperparameters is a great challenge for our desktop-level workstation, only three hyperparameters are selected for the demonstration in this study. Particularly, it should be pointed out that the optimization of hyperparameters facilitated by ISA is also suitable for scenarios with more types of hyperparameters, which involves expanding the final hyperparameter space to include more parameters. For demonstration, the hyperparameters chosen to be optimized are dropout ratio, learning rate, and batch size for the model fitting of ISA-MM-CNNs in the case presented in this paper. The method for hyperparameter optimization is ISA, which has been mentioned in the above section. The influence of different combinations of hyperparameters on model fitting is investigated comparatively, as presented in Fig. 8, with the annotation, which have been demonstrated in Table 2 in detail, of the representative hyperparameters for ISA-MM-CNNs training.

From Fig. 8 it can be observed that different combinations of the hyperparameters have an obvious influence on the model fitting performance according to the accuracy and loss curves in the process of training and testing. In particular, it is easy to notice that the choice of batch size and learning rate has a significant impact on the ability of ISA-MM-CNNs to generalize well on unseen data using CS_CURE_EMI700. For instance, a higher learning rate can speed up convergence but may also increase the risk of oscillations and divergence. Furthermore, the selection of batch size and dropout ratio appears to play a crucial role in determining the capacity of intelligent models to capture complex patterns of the dataset. Therefore, it is essential to carefully tune these hyperparameters in a principled and effective manner, such as the ISA mentioned in this study. Results of this section suggest that careful consideration of these factors can significantly improve the overall performance of the model, allowing it to better adapt to unseen data and make more accurate predictions.

To compare the performance of the ISA-MM-CNNs using the various combinations of the hyperparameters in a more intuitive way, a histogram diagram is plotted, as presented in Fig. 9. In this figure, indicators of the horizontal axis are Accuracy, Precision, Recall, and F1-score, which are employed to evaluate the model performance. The height

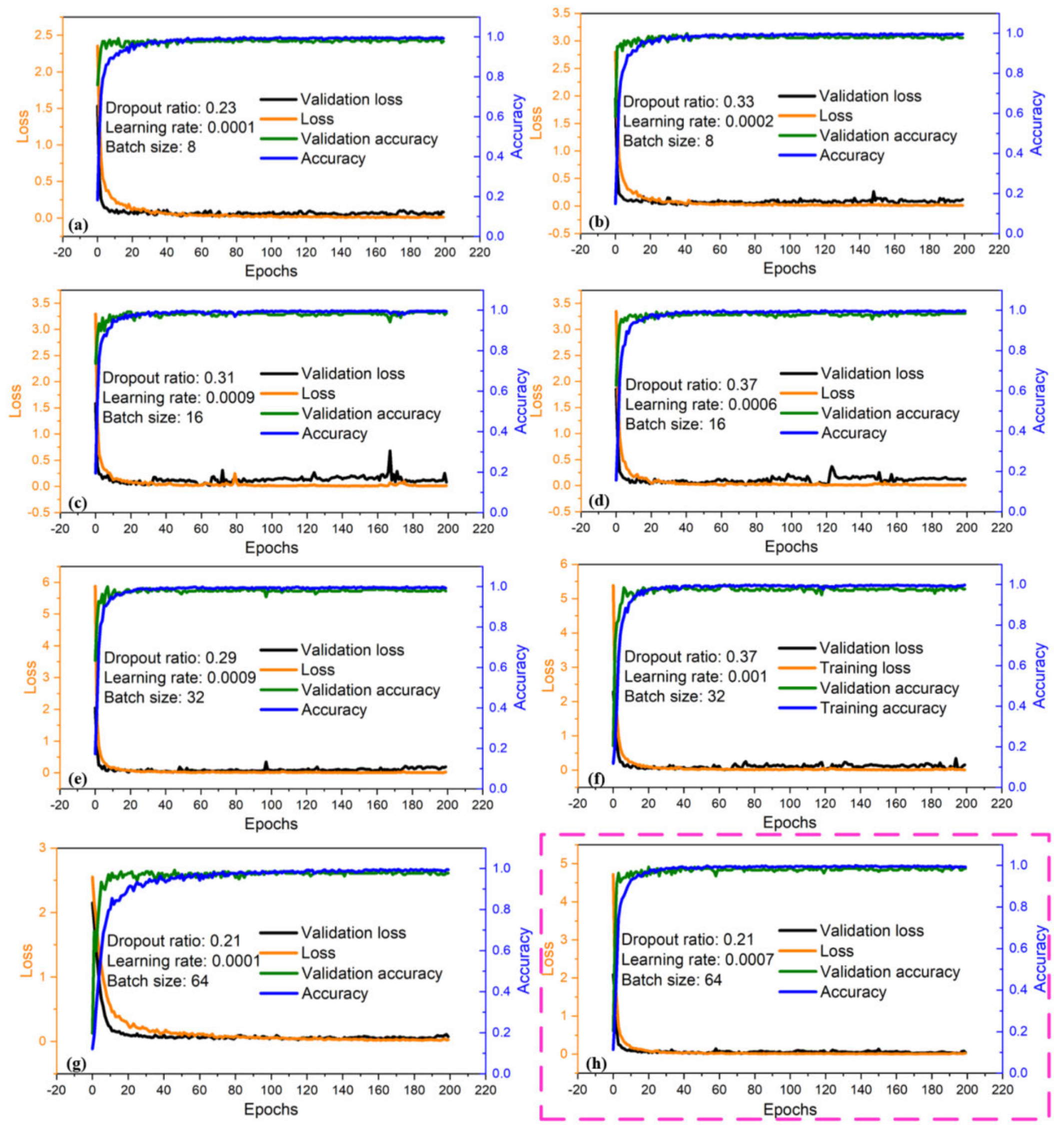

FIGURE 8. Fitting history of ISA-MM-CNNs using CS_CURE_EMI700 dataset with various hyperparameters: (a) HC1, (b) HC2, (c) HC3, (d) HC4, (e) HC5, (f) HC6, (g) HC7, (h) OHP.

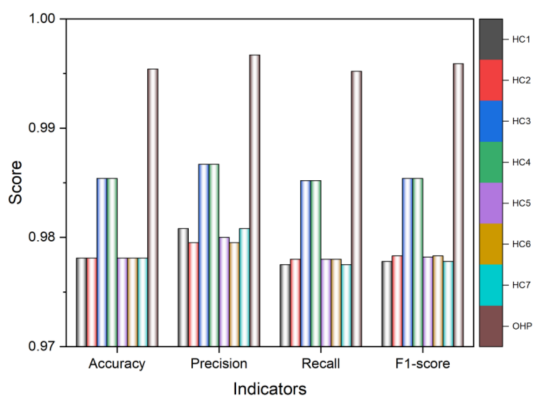

FIGURE 9. Comparison by the histogram including various combinations of hyperparameters.

of the histogram directly corresponds to the score of the trained ISA-MM-CNNs model with different hyperparameter combinations.

The histogram in Fig. 9 provides an intuitive comparison of the ISA-MM-CNNs performance using various hyperparameter combinations, evaluated across Accuracy, Precision, Recall, and F1-score. The results highlight that optimized configurations, such as a learning rate of 7×10^{-4} and a batch size of 64, consistently deliver superior performance across all metrics, indicating an effective balance between learning efficiency and stability. This comprehensive evaluation reveals that the most effective hyperparameter combinations are those that perform well across all four metrics, guiding future experiments toward configurations that ensure high accuracy, precise predictions, comprehensive recall, and robust overall performance.

B. CONFUSION MATRIX OF ISA-MM-CNNs FOR CURING PROCESS EVALUATION

The confusion matrix (CM) is one heatmap used to evaluate the performance of a classification algorithm by showing

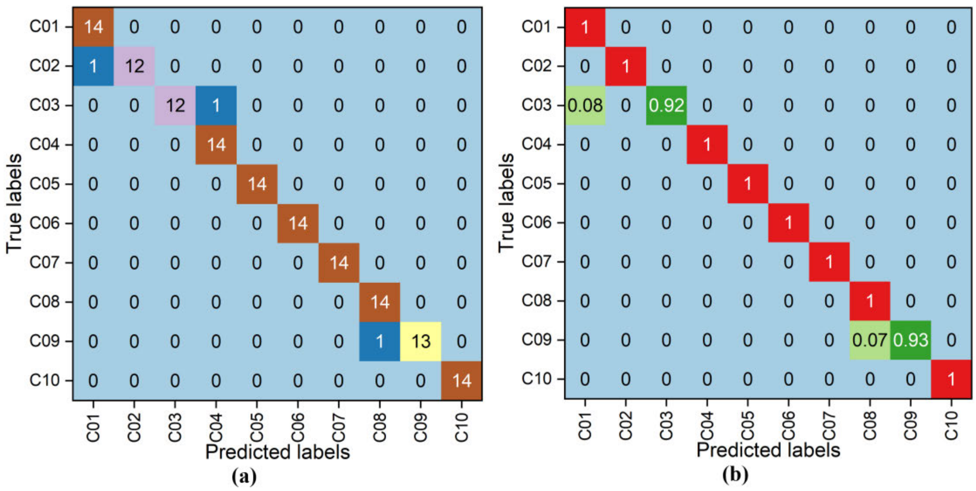

FIGURE 10. **Diagram of classification results applying ISA-MM-CNNs to CS_CURE_EMI700 dataset: (a) Non-normalized CM, (b) Normalized CM.**

the actual versus predicted classifications. It helps identify not only the accuracy of the model but also the errors it makes. This study employs the CM plots to depict the classification result of ISA-MM-CNNs on the dataset ''CS_CURE_EMI700'', as shown in Fig. 10.

Fig. 10 shows two CM plots labeled (a) and (b), which illustrate the performance of a classification model across ten categories, ranging from C01 to C10. Fig. 10 (a) presents the raw sample counts for true versus predicted labels. The diagonal entries represent the number of correctly classified samples for each category, such as 14 samples for C01, whereas off-diagonal entries indicate misclassifications, like 1 sample of C01 being misclassified as C02. Fig. 10 (b) conveys classification accuracy and error rates. Diagonal values denote the accuracy for each class, with C01 achieving 100% accuracy (1.00) and C03 achieving 92% accuracy (0.92). Off-diagonal values represent the proportion of misclassified samples, exemplified by 8% of C03 samples being misclassified as C04 (0.08). These CM plots collectively reveal that the model performs well, with most errors occurring between adjacent categories. Overall, Fig. 10 (a) provides detailed counts of correct and incorrect classifications, while Fig. 10 (b) offers a clearer perspective on the accuracy of ISA-MM-CNNs and error distribution, facilitating a comprehensive evaluation of its performance.

From the perspective of evaluating the curing degree, Fig. 10 reveals that the proposed ISA-MM-CNNs model performs exceptionally well in accurately assessing the degree of cure for composite materials, particularly in the mid to fully cured stages (C04 to C10), where it shows perfect accuracy, which indicates that the characteristics of composite materials in these stages are distinct and easily recognized by the proposed ISA-MM-CNNs model. However, a slight decrease in accuracy for early cure stages (C02 and C03) is also observed, with some misclassification occurring between adjacent stages. This suggests that the features of composite materials in the early stages are less distinct, leading to overlap. Additionally, there is minor misclassification in the late cure stage (C09) with the fully cured stage (C10), which is expected as the material properties in these stages become very similar. Overall, the ISA-MM-CNNs model is highly effective in assessing the cure degree, with opportunities for minor improvements in the early and late stages to enhance accuracy further.

C. COMPARISON BETWEEN ISA-MM-CNNS AND OPEN-SOURCE MODELS

In order to demonstrate the performance and effectiveness of the proposed ISA-MM-CNNs approach in the application of evaluating the composite curing degree, the comparison between ISA-MM-CNNs with the open-source models is conducted, as presented in Fig. 11. This figure comprises three bar charts, which are Fig. 11 (a), (b), and (c), comparing the performance across four key evaluation indicators: Accuracy, Precision, Recall, and F1-score. To be more specific, the networks for comparison are ISA-MM-CNNs, InceptionResNetV2, InceptionV3, MobileNetV2, ResNet50V2, ResNet152V2, VGG16, VGG19, and Xception. Each model is represented by a distinct color, as indicated in the legend on the right side of each chart. Across all three subfigures of Fig. 11, ISA-MM-CNNs consistently outperform the other models in all metrics. In Fig. 11 (a), ISA-MM-CNNs achieve the highest scores in the above-mentioned four indices, implying fewer false positives and negatives. Fig. 11 (b) reinforces this trend, with ISA-MM-CNNs demonstrating superior performance, although the gap in precision is slightly narrower compared to Fig. 11 (a). Fig. 11 (c) shows ISA-MM-CNNs achieving near-perfect accuracy and exceptional recall, highlighting their effectiveness across different tasks or datasets.

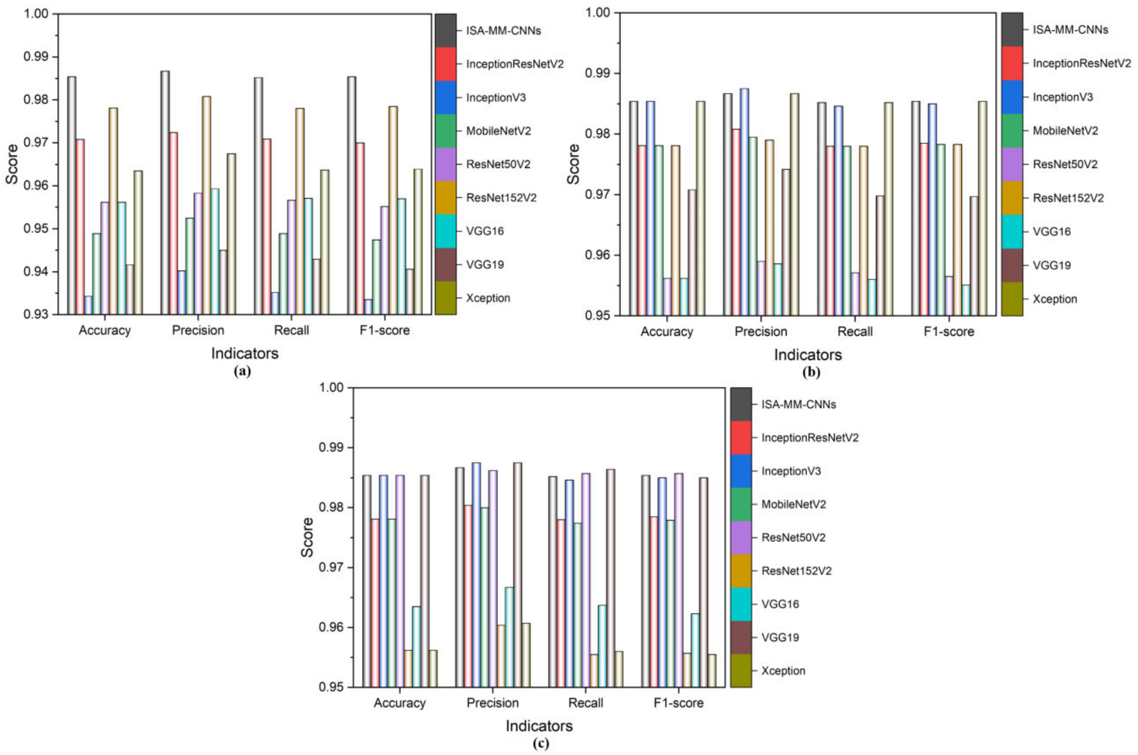

FIGURE 11. Comparison between the proposed ISA-MM-CNNs and the open-source models.

Overall, on the dataset of "CS_CURE_EMI700" built in our laboratory, the high performance of the proposed ISA-MM-CNNs across all indicators and figures underscores their robustness and reliability when employed in the scenarios relevant to the composite curing. Besides, InceptionResNetV2 and InceptionV3 also perform well but often rank just below ISA-MM-CNNs, particularly in accuracy and precision. Other models, including MobileNetV2, ResNet variants, VGG16, VGG19, and Xception, show competitive performance but consistently lag behind ISA-MM-CNNs and the Inception variants. These observations indicate that ISA-MM-CNNs are highly effective for tasks requiring high accuracy and precision, making the proposed approach a preferred choice in these scenarios.

V. CONCLUSION

This study developed an ISA-MM-CNNs paradigm designed for EMI-based monitoring of the composite curing process. The findings highlight that integrating importance sampling with the multi-modal learning method significantly enhances the accuracy and efficiency of CNN models in processing complex EMI signals.

The proposed ISA-MM-CNNs paradigm effectively addresses critical challenges such as data heterogeneity, class imbalance, and computational complexity, demonstrating superior performance compared to existing approaches. By focusing training efforts on informative samples and capturing complementary information from different EMI signal modalities, the ISA-MM-CNNs provide a robust and efficient solution for real-time, non-destructive evaluation of composite curing processes. Nevertheless, this study also has limitations, including the reliance on synthetic datasets and the necessity for further validation using diverse, real-world data. Future research should explore the application of ISA-MM-CNNs in various industrial settings and investigate the integration of additional sensor modalities to further enhance the robustness of the monitoring system.

Summarily, this study offers a promising solution for enhancing the quality and efficiency of composite structure manufacturing processes, paving the way for innovative advancements in composite structure monitoring. It suggests that ISA-MM-CNNs hold significant potential in addressing the limitations of conventional methods and exploiting the synergies between different signal modalities.

REFERENCES

[1] B. Wang, S. Fan, J. Chen, W. Yang, W. Liu, and Y. Li, "A review on prediction and control of curing process-induced deformation of continuous fiber-reinforced thermosetting composite structures," *Compos. A, Appl. Sci. Manuf.*, vol. 165, Feb. 2023, Art. no. 107321.

[2] C. Ji, H. Huang, T. Wang, and Q. Huang, "Recent advances and future trends in processing methods and characterization technologies of aluminum foam composite structures: A review," *J. Manuf. Processes*, vol. 93, pp. 116–152, May 2023.

[3] P. Cao, S. Zhang, Z. Wang, and K. Zhou, "Damage identification using piezoelectric electromechanical impedance: A brief review from a numerical framework perspective," *Structures*, vol. 50, pp. 1906–1921, Apr. 2023.

[4] P. E. C. Pereira, S. W. F. de Rezende, H. C. Fernandes, J. D. R. V. de Moura Junior, and R. M. F. Neto, "On damage location techniques and future prospects for industrial applications utilizing the electromechanical impedance method: A systematic review," *J. Brazilian Soc. Mech. Sci. Eng.*, vol. 46, no. 5, p. 311, May 2024.

[5] A. F. G. Tenreiro, A. M. Lopes, and L. F. da Silva, "A review of structural health monitoring of bonded structures using electromechanical impedance spectroscopy," *Struct. Health Monitor.*, vol. 21, no. 2, pp. 228–249, Mar. 2022.

[6] F. G. Baptista, J. V. Filho, and D. J. Inman, "Real-time multi-sensors measurement system with temperature effects compensation for impedance-based structural health monitoring," *Struct. Health Monitor.*, vol. 11, no. 2, pp. 173–186, Mar. 2012.

[7] D. F. Gonçalves, F. B. A. de Freitas, A. A. Cavalini Jr., R. M. F. Neto, and V. Steffen Jr., "Machine learning and electromechanical impedance applied in the structural health monitoring," in *Proc. 27th Int. Congr. Mech. Eng.*, 2023, pp. 487–495.

[8] D. Sahm and D. Pak, "Influence of temperature and preload force on capacitance and electromechanical impedance of lead zirconate titanate piezoelectric wafer active sensors for structural health monitoring of bolts," *Appl. Phys. A, Solids Surf.*, vol. 130, no. 3, p. 156, Mar. 2024.

[9] M. K. Dahl, J. H. Hire, M. Zamani, and F. Moradi, "Multimodal temperature sensing using electromechanical impedance (EMI) for structural health monitoring," *IEEE Sensors J.*, vol. 24, no. 3, pp. 3457–3464, Mar. 2024.

[10] W. A. Agha, S. Pal, and N. Dev, "Challenges for structural health monitoring of concrete curing using piezoelectric sensor and electromechanical impedance (EMI) technique: A critical review," *Mater. Today, Proc.*, Jul. 2023, Art. no. S2214785323038464, doi: 10.1016/j.matpr.2023.06.451.

[11] W. Luo, T. Liu, W. Li, and M. Luo, "Pitting corrosion prediction based on electromechanical impedance and convolutional neural networks," *Struct. Health Monitor.*, vol. 22, no. 3, pp. 1647–1664, May 2023.

[12] D. Ai and J. Cheng, "A deep learning approach for electromechanical impedance based concrete structural damage quantification using two-dimensional convolutional neural network," *Mech. Syst. Signal Process.*, vol. 183, 2023.

[13] Z. Wang and L. Qin, "Research of structural health intelligent monitoring technology based on PZT and electromechanical impedance method," in *Proc. 7th Int. Conf. Cyber Secur. Inf. Eng.*, Sep. 2022, pp. 497–501.

[14] W. S. Na and J. Baek, "A review of the piezoelectric electromechanical impedance based structural health monitoring technique for engineering structures," *Sensors*, vol. 18, no. 5, p. 1307, Apr. 2018.

[15] J. Zhu, J. Wen, Z. Han, M. M.-P. Ho, Z. Lan, Y. Wang, and X. Qing, "Impact energy assessment of sandwich composites using an ensemble approach boosted by deep learning and electromechanical impedance," *Smart Mater. Struct.*, vol. 32, no. 9, Sep. 2023, Art. no. 095019.

[16] F. Jiang, Z. Guan, X. Wang, Z. Li, R. Tan, and C. Qiu, "Study on prediction of compression performance of composite laminates after impact based on convolutional neural networks," *Appl. Compos. Mater.*, vol. 28, no. 4, pp. 1153–1173, Aug. 2021.

[17] H. Li, D. Ai, H. Zhu, and H. Luo, "Integrated electromechanical impedance technique with convolutional neural network for concrete structural damage quantification under varied temperatures," *Mech. Syst. Signal Process.*, vol. 152, May 2021, Art. no. 107467.

[18] R. Janeliukstis and D. Mironovs, "Smart composite structures with embedded sensors for load and damage monitoring—A review," *Mech. Compos. Mater.*, vol. 57, no. 2, pp. 131–152, May 2021.

[19] B. Feng, J. Zhang, S. Chen, H. Liang, and Y. Kang, "Impact localization in composite structures with guided wave and 1D convolutional neural network," *Res. Rev. J. Nondestruct. Test.*, vol. 1, no. 1, pp. 1–12, Aug. 2023.

[20] S. W. F. de Rezende, J. D. R. V. de Moura, R. M. F. Neto, C. A. Gallo, and V. Steffen, "Convolutional neural network and impedance-based SHM applied to damage detection," *Eng. Res. Exp.*, vol. 2, no. 3, Sep. 2020, Art. no. 035031.

[21] S. Goossens, T. Geernaert, Z. S. Khodaei, E. Karachalios, D. Saenz-Castillo, and F. Berghmans, "Barely visible impact damage detection and location on composite materials by surface-mounted and embedded aerospace-compatible optical fibre Bragg grating sensors," *Proc. SPIE*, vol. 11354, p. 17, Apr. 2020.

[22] B. Zamorano and N. Elvin, "Passive high-speed impact damage assessment in composite panels using embedded piezoelectric sensors," *J. Intell. Mater. Syst. Struct.*, vol. 27, no. 1, pp. 104–116, Jan. 2016.

[23] F. Du, S. Wu, C. Xu, Z. Yang, and Z. Su, "Electromechanical impedance temperature compensation and bolt loosening monitoring based on modified UNet and multitask learning," *IEEE Sensors J.*, vol. 23, no. 5, pp. 4556–4567, Mar. 2023.

[24] L. Parida, S. Moharana, V. M. Ferreira, S. K. Giri, and G. Ascensão, "A novel CNN-LSTM hybrid model for prediction of electro-mechanical impedance signal based bond strength monitoring," *Sensors*, vol. 22, no. 24, p. 9920, Dec. 2022.

[25] S. P. Caldwell and D. W. Radford, "Composite single lap shear joint integrity monitoring via embedded electromechanical impedance sensors," *J. Compos. Sci.*, vol. 7, no. 2, p. 53, Feb. 2023.

[26] A. Pisharody and D. E. Smith, "An experimental and numerical investigation into the effects of bond line thickness variations on the strength of composite bonded joints," *Compos. Struct.*, vol. 279, Jan. 2022, Art. no. 114789.

[27] V. Giurgiutiu and A. Zagrai, "Damage detection in thin plates and aerospace structures with the electro-mechanical impedance method," *Struct. Health Monitor.*, vol. 4, no. 2, pp. 99–118, Jun. 2005.

[28] A. Scott and A. Metzler, "A general importance sampling algorithm for estimating portfolio loss probabilities in linear factor models," *Insurance, Math. Econ.*, vol. 64, pp. 279–293, Sep. 2015.

[29] W. Li and G. Lin, "An adaptive importance sampling algorithm for Bayesian inversion with multimodal distributions," *J. Comput. Phys.*, vol. 294, pp. 173–190, Aug. 2015.

[30] X. Yuan, Z. Lu, C. Zhou, and Z. Yue, "A novel adaptive importance sampling algorithm based on Markov chain and low-discrepancy sequence," *Aerosp. Sci. Technol.*, vol. 29, no. 1, pp. 253–261, Aug. 2013.

[31] S. T. Tokdar and R. E. Kass, "Importance sampling: A review," *WIREs Comput. Statist.*, vol. 2, no. 1, pp. 54–60, 2010.

[32] A. Tabandeh, G. Jia, and P. Gardoni, "A review and assessment of importance sampling methods for reliability analysis," *Struct. Saf.*, vol. 97, Jul. 2022, Art. no. 102216.

[33] H. N. Nagaraja, "Inference in hidden Markov models," *Technometrics*, vol. 48, pp. 574–577, Apr. 2006.

[34] Y. Zhang, K. Gong, K. Zhang, H. Li, Y. Qiao, W. Ouyang, and X. Yue, "Meta-transformer: A unified framework for multimodal learning," 2023, *arXiv:2307.10802*.

[35] P. Xu, X. Zhu, and D. A. Clifton, "Multimodal learning with transformers: A survey," *IEEE Trans. Pattern Anal. Mach. Intell.*, vol. 45, no. 10, pp. 12113–12132, Oct. 2023.

XIN ZHAO received the Ph.D. degree in materials physics and in chemistry from Sichuan University, Chengdu, China, in 2009.

He is currently a Professor with the School of Aeronautical Engineering, Civil Aviation Flight University of China, Sichuan, China, where he is also the Dean of the Graduate Office and the Director of the Discipline Construction Office. His research interests include advanced aviation materials, aircraft anti-deicing technologies, and carbon-neutral technologies. He has published over 50 research articles, including 12 SCI-indexed articles and has authored two textbooks. He has led or participated in several provincial and ministerial research projects, applied for five national patents, and received Sichuan Province Award for Excellence in Graduate Education.

ZEYUAN GAO was born in Baoji, Shaanxi, China, in 2001. He received the bachelor's degree in aircraft power engineering from the Civil Aviation Flight University of China, Sichuan, China, in 2023, where he is currently pursuing the master's degree.

His major field of study includes structural health monitoring and 3D-printed composite material structures. He has participated in research projects on additive manufacturing and composite materials, focusing on advanced materials and monitoring techniques to enhance aerospace structure performance and reliability.

MENG LI was born in Chengdu, Sichuan, China, in 1978. He received the Ph.D. degree in material science from Sichuan University, in 2008.

Since 2015, he has been a Professor and a Master's Supervisor with the College of Aviation Engineering, Civil Aviation Flight University of China. His research interests include aerospace functional materials and aircraft maintenance engineering.

Prof. Li is a member of the Society for the Advancement of Material and Process Engineering. He is a Reviewer of the following international journals: *Polymer Engineering & Science*, *International Journal of Hydrogen Energy*, *Powder Metallurgy*, and *Physica Status Solidi (RRL)—Rapid Research Letter*.

ZHIBIN HAN was born in Zhangzhou, Fujian, China, in 1993. He received the B.S. and M.S. degrees from the School of Aerospace Engineering, Xiamen University, in 2016 and 2019, respectively, and the Ph.D. degree from the Department of Mechanical and Automation Engineering, The Chinese University of Hong Kong.

Currently, he is a Postdoctoral Researcher with the Faculty of Aerospace Engineering, Technology University of Delft, The Netherlands. He has published over 20 articles and several patents. His research interests include the carbon fiber-reinforced polymer, structural batteries, engine health management, sensors, and machine learning.

JIANJIAN ZHU received the Ph.D. degree in aerospace engineering from Xiamen University, Xiamen, China.

His major field of study is aircraft health management and intelligent structures. Currently, he is an Associate Professor with the Civil Aviation Flight University of China, Sichuan, China, where he leads the ''Aircraft Health Management and Intelligent Structures'' Research Team. He has authored or co-authored more than 40 academic articles in SCI and EI journals and holds over ten patents. His current research interests include structural health monitoring, 3D printing/additive manufacturing, aerospace composite materials, and artificial intelligence.

Dr. Zhu is a member of Chinese Society for Composite Materials and Chinese Society of Instrumentation. He serves as an Expert for the National Natural Science Foundation of China and has reviewed articles for journals, such as *Mechanical Systems and Signal Processing* and *Composite Structures*.